Recombination and spin relaxation of hydrogen and deuterium atoms in molecular crystals

A. S. Iskovskikh, A. Ya. Katunin, I. I. Lukashevich, V. V. Sklyarevskiĭ, V. V. Suraev, V. V. Filippov, N. I. Filippov, and V. A. Shevtsov

I. V. Kurchatov Atomic Energy Institute

The temperature dependence of the absolute recombination rate constant is measured for deuterium atoms in a D_2 crystal. Thermally activated atomic diffusion is shown to be responsible for recombination at higher temperatures $T \gtrsim 7.5$ K. For $T \lesssim 7$ K, the observed temperature dependence $K_D \propto T^9$ of the rate constant suggests that at these temperatures the recombination is due to two-phonon quantum diffusion of deuterium atoms in the D_2 crystal. The experimental results for D atoms in a D_2 matrix are compared with the temperature dependence of the absolute recombination rate constant for H atoms in an H_2 matrix. The longitudinal electron relaxation time T_e (10–100 s) for hydrogen atom impurities in a para-H_2 crystal is shown to coincide with the nuclear relaxation time. The monotonic behavior, approximately as $T_e \propto H^2$, with increasing magnetic field H indicates that the atoms diffuse quite rapidly in the crystal (several orders of magnitude faster than the rates obtained from the recombination data).

1. INTRODUCTION

The quantum diffusion of light-weight atoms in crystals is an important area of research in low-temperature physics. ^{3}He and ^{4}He solid solutions were the first (and until recently, the only) systems to clearly exhibit the quantum diffusion of impurity atoms predicted theoretically by Andreev and Lifshitz[1] and confirmed experimentally by Grigor'ev, Esl'son, and Mikheev.[2] This discovery stimulated further theoretical and experimental work[3,4] which resulted in the prediction and experimental observation of a variety of novel effects, including the self-localization of quantum impurities in quantum crystals.

It was later found[5,6] that quantum diffusion of atomic impurities also occurs in H_2 crystals containing *H* impurity atoms. Unlike the ^{3}He–^{4}He system, the H–H_2 system is metastable because the atoms recombine at a rate that depends on how closely they approach one another by diffusion. This thus provides a way to analyze the atomic diffusion by using electron paramagnetic resonance (EPR) to measure how the atomic concentration changes with time. The distinctive feature of this type of "recombination" diffusion is that it requires pairs of atoms to approach each other to within distances comparable to the lattice constant. The perturbation of the energy levels for atoms in adjacent positions increases as the atoms move closer together.

The recombination of atoms in systems with quantum diffusion was analyzed theoretically by Kagan and Maksimov.[7] Their theory gives a satisfactory explanation for the linear temperature dependence of the recombination rate constant for H atoms in H_2 crystals for $1.3 \lesssim T \lesssim 4$ K. They also pointed out that recombination diffusion should be much slower than "spatial" diffusion of atoms, because in the latter case the atoms can move in directions that correspond to a minimal disruption of the energy levels. Recent data[8] indicate that the spatial diffusion of H atoms in a para-hydrogen crystal is quite rapid. We will discuss this more fully in Sec. 7 below.

The question of what happens when the H–H_2 system is replaced by the isotopic analog D–D_2 is of natural interest. It was first observed in Ref. 9 that the temperature dependence $K_D(T)$ of the recombination constant for D atoms in a D_2 matrix is not of the activation type. In the present paper we report data on $K_D(T)$ for D atoms in a D_2 matrix for $T = 4.2$–9.5 K. We show that for $4.2 < T < 7$ K, the temperature dependence $K_D(T)$ is of the form $K_D \propto T^9$, which suggests that the recombination is due to quantum diffusion of D atoms in which two-phonon processes participate. The dependences $K_H(T)$ and $K_D(T)$ for H–H_2 and D–D_2 systems are compared.

2. EXPERIMENT

The experimental technique for analyzing the recombination of D atoms in a D_2 matrix was in many respects similar to the one used previously in Refs. 5 and 6. Figure 1 shows a sketch of the low-temperature portion of the experimental device and the system for producing and transporting the atomic-molecular beam.

The mixture of atoms and molecules generated in the rf dissociator 8 was transported over a quartz atom guide 6 to the working zone of the cryostat. The beam of atoms and molecules then condensed on a cold ($T \lesssim 2$ K) single-crystal quartz or sapphire substrate 2 contained in the microwave cavity of the EPR spectrometer, which operated at wavelengths in the 3-cm range. The spectrometer measured the number of atoms in the condensate and its time dependence during recombination.

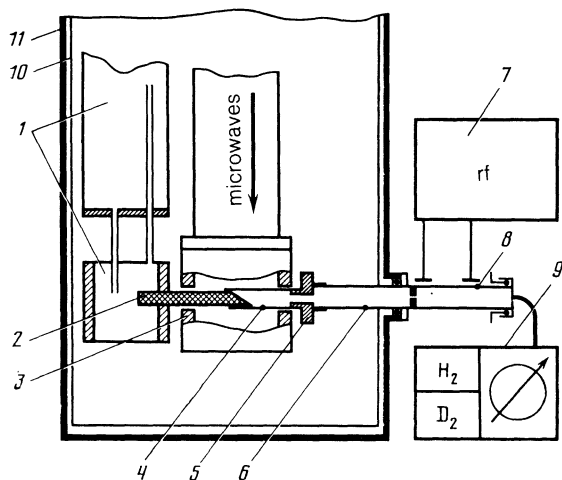Two types of atom guides were used in the experiments. The terminal section of the guide in the first case was "open"

FIG. 1. Low-temperature portion of the experimental device, and system for producing the atom-molecule mixture: 1) helium vessel ($T \gtrsim 1.3$ K; 2) cooled substrate (single-crystal quartz); 3) microwave cavity of EPR spectrometer; 4) lavsan tube; 5) adapter; 6) atom guide (quartz); 7) rf oscillator; 8) dissociator (quartz); 9) system for measuring and adjusting the inflow of hydrogen; 10) radiation screen ($T \approx 77$ K); 11) cryostat case.

FIG. 2. a) Sketch showing D-atom energy levels in a magnetic field with different projections of the nuclear (I) and electron (S) spins. b) First derivatives of the hyperfine components of the EPR spectrum for D atoms in a D_2 matrix at several microwave powers P($P = 1$ corresponds to ~ 10 μW).

to permit the atom-molecule beam to pass unobstructed through the guide/substrate section. As a result, an unknown percentage of the beam was scattered, and only an upper bound could be given for the number of molecules in the specimen. Since the atomic concentration was unknown, what was actually measured was the ratio $K(T)/K(T_0)$ of the recombination rates in the same specimen, where T_0 is some fixed temperature. Such an open configuration was used in Refs. 5, 6 to study the recombination of hydrogen atoms in an H_2 matrix, and also in Ref. 10, where the first results on deuterium recombination in D_2 were reported.

The second type of atom guide was "closed" in order to eliminate scattering of molecules on their way to the substrate. This was done by using a lavsan (plastic) tube 4 of thickness $\sim 10 \mu$m to hermetically connect the substrate 2 to the quartz atom guide 6 by means of a Teflon adapter 5. The lavsan tube also served to thermally decouple the substrate from the comparatively hot end of the guide. Because of the low thermal conductivity of the lavsan, most of the lateral surface of the tube 4 was warm enough to keep the D_2 molecules from condensing. (In a control experiment, a sensor attached to the side of the tube at a distance ~ 3 mm from the adapter gave a reading of ~ 70 K even in the absence of heating by the atom-molecule beam.) We may thus assume that in this case, nearly all the molecules reaching the dissociator are condensed on the substrate 2. The "closed" geometry thus enables one to measure the number of molecules and hence the atomic concentration and absolute recombination rates in the specimen. The initial D atom concentrations reached $9 \cdot 10^{19}$ cm^{-3} ($\sim 0.3\%$).

We also used a closed atom guide in control experiments to verify that none of the D_2 (H_2) molecules were vaporized and thereby ensured that the number of molecules in the specimens remained constant for several hours. The behavior of the EPR signal (which is proportional to the
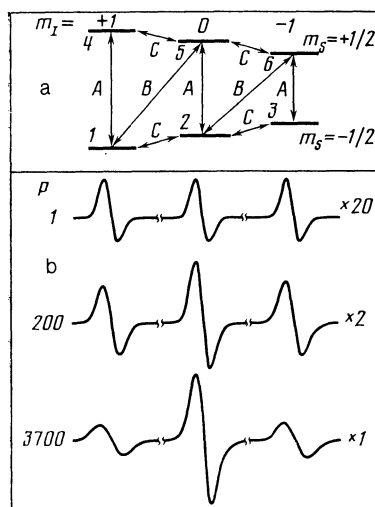
number of atoms) therefore accurately reflected the behavior of the atomic concentration in the specimen.

3. SPECTRA FOR DEUTERIUM ATOMS IN A D_2 MATRIX

3.1. Electron and nuclear relaxation for deuterium atoms

Figure 2a shows a diagram of the energy levels for a deuterium atom in a magnetic field. The transitions with $\Delta m_S = 1$, $\Delta m_I = 0$ give rise to three hyperfine structure lines of equal intensity in the deuterium EPR spectrum, and this is also observed even when the transitions are not saturated (Fig. 2b, $P = 1$). As the microwave power fed to the cavity increases, we found (as in Ref. 11) that the intensities of the central and satellite lines began to differ significantly. The figures in Ref. 12 also reveal a difference in the intensities of the hyperfine lines for the D–D_2 system. Figure 2b shows that the degree of saturation for the satellite lines is considerably greater than for the central line. The differences in the saturations show up more clearly in Fig. 3, which shows logarithmic plots of the amplitudes $A(P)$ and widths $\Delta H(P)$ of the first derivative of each of the three lines in the EPR absorption spectrum, where P is the microwave power. For small P we have the dependence $\Delta H = $ const and $A \propto P^{1/2}$, as expected for unsaturated EPR transitions. For large P, the saturation for each of the lines can be judged by the deviation from this dependence, as well as by the line broadening. We note that the line intensities are independent of the saturation time, i.e., they do not change with time while the populations of the levels 1–6 (Fig. 2a) are being recorded.

It is natural to attribute the unequal intensities of the central and satellite lines to differences in the effective relaxation rates for the transitions between the sublevel pairs. We believe that such differences can arise only if the relaxation rates for the electron and nuclear spins in the deuterium atom are comparable (processes A and C in Fig. 2a). In this case, the increase in the effective relaxation rate for sublevel

$\left|\frac{dX''}{dH}\right|$

ΔH

A

H

1

0

−1

ΔH,Oe
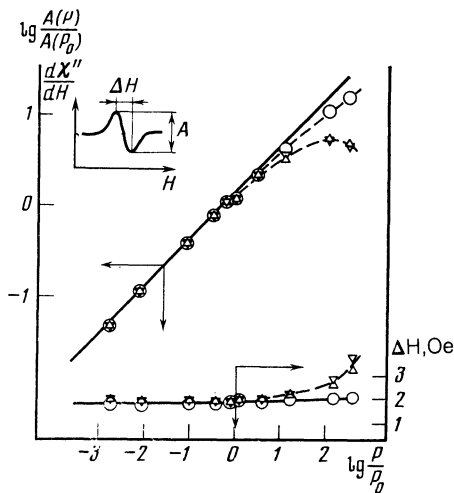
3

2

1

−3 −2 −1 0 1 2 lg $\frac{P}{P_0}$

FIG. 3. Amplitude A and width ΔH of the first derivative of the hyperfine EPR components for deuterium atoms as function of the microwave power $(P_0 \sim 10\,\mu\text{W}$: ∇, $m_I = +1$; O, $m_I = 0$; Δ, $m_I = -1$.

pairs via additional closed chains of the type C-A-C should be greater for the 2–5 transition than for the 1–4 and 3–6 transitions. The maximum ratio of the steady-state population differences, which is equal to $(n_2 - n_5)/(n_1 - n_4) = 1.25$, is reached in the limit $P \to \infty$ and corresponds to a relaxation time ratio T_C/T_A equal to 0.5.

It is easy to show that under steady-state conditions, the "forbidden" electron-nucleus relaxation processes (B in Fig. 2a) cannot cause the effective relaxation rates for the 2–5 and 1–4 (3–6) to differ.

The considerable difference in the saturations of the central and satellite lines in the EPR spectrum for D–D$_2$ observed in our experiments thus indicates that the nuclear and electron spin relaxation times for atomic deuterium are comparable. This is somewhat unexpected, since the matrix element for the C transitions is less than the matrix element for the A transitions by a factor of $g_e\beta_e H/hA$ (here $g_e\beta_e H$ and hA are the Zeeman and hyperfine interaction energies for the electron spin in atomic deuterium). Other conditions being the same, we would thus expect the nuclear relaxation time to be ~ 3600 times longer than the electron relaxation time.

Rapid nuclear relaxation for D atoms in a D$_2$ matrix was also found in Ref. 13, where relaxation measurements under time-dependent conditions gave comparable values for the electron and nuclear relaxation times.

We note that the electron and nuclear relaxation times could become comparable if, e.g., the electron relaxation times depend quadratically on the magnetic field, $T_A \propto H^2$. Since for magnetic fields in the range investigated the nuclei relax mostly through mixed states in the hyperfine energy level structure, we then obtain

$$T_C^{-1} = \frac{\text{const}}{(hA)^2}\left(\frac{hA}{g_e\beta_e H}\right)^2 = \frac{\text{const}}{(g_e\beta_e H)^2} = T_A^{-1}.$$

We will show in Sec. 7 that this is in fact the situation for hydrogen atoms in a para-H$_2$ crystal. In particular, the dependence $T_A \propto H^2$ in this case indicates that no phonons are

involved in the relaxation mechanism; such a dependence could occur if the quantum diffusion of the H atoms is quite rapid. Unfortunately, the lack of additional experimental data (on the values of T_A and their dependence on H, for example) precludes a definitive treatment of the equality $T_C \approx T_A$ for D atoms in a D$_2$ matrix at the present time.

3.2 Line widths for deuterium atoms in a D$_2$ matrix

It was shown in Ref. 14 that in the analogous H − H$_2$ system, the absorption line for the hydrogen atoms is nearly Gaussian with a halfwidth ΔH that increases rapidly as T rises from 4.5 to 5.75 K. In our experiments, the deuterium lineshapes were appreciably nongaussian; indeed, the observed ratio $M_4/3M_2^2$ of the fourth and second moments of the line was equal to 1.4 ± 0.1 (this should be 1 for a Gaussian line and should approach infinity for a Lorentzian). The lineshape can be approximated quite closely as a convolution of Gaussian and Lorentzian distribution functions.

The initial linewidth immediately upon formation of the specimens was between 1.3 and 2.2 Oe (the instrument width was ~ 0.1 Oe). As the atomic concentration dropped due to recombination, ΔH decreased and approached the value $\Delta H(0) = 1.4 \pm 0.1$ Oe in the limit $n_D \to 0$. In all cases, the EPR linewidth for the deuterium atoms was independent of temperature for $1.5 < T < 8.5$ K.

4. RECOMBINATION OF DEUTERIUM ATOMS IN A D$_2$ MATRIX

As in the H–H$_2$ specimens,[5,6] the equation

$$dn/dt = -2K_D(T)n^2 \qquad (1)$$

in most cases accurately describes how the D atom concentration decreases with time when the sample temperature is kept constant. Here $K_D(T)$ is the recombination rate constant. The experimental dependence between the variables $1/n$ and t should thus be linear, with slope equal to $2K_D(T)$. The characteristic time for the concentration to drop by 50% is $\tau_{1/2} = (2K_D n_0)^{-1}$.

We ran some control experiments which demonstrated that $K_D(T)$ was unaffected by recombination heating of the D–D$_2$ specimens.[15] This was necessary, because the concentration of D atoms in the D$_2$ was roughly an order of magnitude higher than in the H–H$_2$ specimens investigated previously. Nevertheless, it should be noted that in some cases a departure from the dependence (1) was observed; these cases were eliminated from further consideration.

The error in the K_D values was determined by the $\sim 40\%$ error in measuring the absolute atomic concentrations in the specimens and by errors in measuring the decrease in the concentration at a fixed temperature. The errors in $1/T$ at each point (Fig. 4) are due primarily to uncontrolled fluctuations in the temperature. The accuracy of the measured absolute rate constants and atomic concentrations is discussed in greater detail in Ref. 15.

4.1 Temperature dependence of the absolute rates $K_D(T)$.

Figure 4 plots the dependence $K_D(T)$ in log K_D, $1/T$ coordinates. The values were obtained from 11 different D–
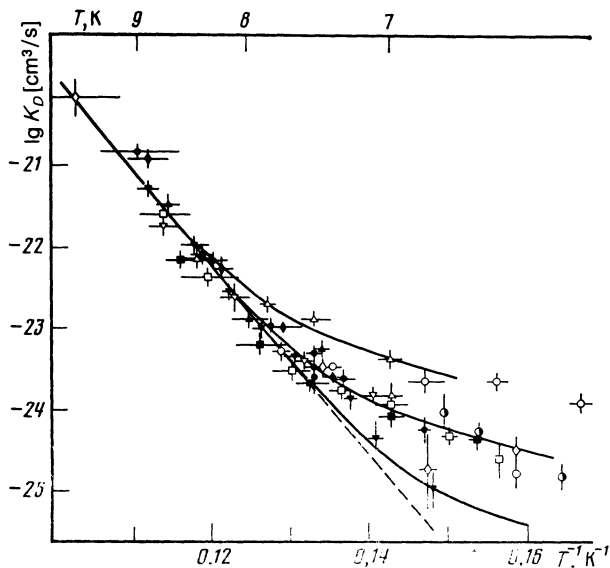
FIG. 4. Temperature dependence of the absolute recombination rate constants for deuterium atoms in a D_2 matrix (different symbols refer to different specimens).

D_2 specimens using a closed atom guide; here and throughout, the absolute rates are expressed in cm^3/s. We see that there are two temperature regions. For $T > 7.5$ K, the values K_D found for the different specimens coincide to within the experimental error, and the time dependence of the recombination rate is given by

$$K_D = K_D^0 \exp{(-E_a/T)}. \qquad (2)$$

At lower temperatures $T < 7.5$ K, Eq. (2) starts to overestimate K_D. However, the size of the error differs from one specimen to the next, and even though K_D decreases monotonically with T in all cases, this gives rise to a fan-like spread in the curves $K_D(T)$ whose magnitude is much greater than the experimental error. Consequently the experimental curves $K_D(T)$ for $T < 7.5$ K cannot be described by a single curve for all of the specimens. We therefore approximated the data by a formula of the type

$$K_D(T) = K_D^0 \exp{(-E_a/T)} + BT^n \qquad (3)$$

in which K_D^0, E_a, and n have fixed values but B is allowed to vary from one specimen to the next so as to accommodate the spread in K_D at low temperatures. The following values were used:

$$\lg B = -30.8 \div -31.5 \div -32.4,$$
$$\lg K_D^0 = -8.2 \pm 1.5, \quad E_a = 270 \pm 30, \qquad (4)$$
$$n = 8.8 \pm 0.6.$$

The solid lines in Fig. 4 plot (3), (4); the deviation from (3), (4) is appreciable only for one specimen (denoted by the open circle in Fig. 4).

We also note that the low-temperature portions of $K_D(T)$ for each specimen can be described by an activation dependence of the form (2) as well as by a power law (3). However, this yields activation energies ~ 50 K and leads to anomalously small values for the preexponential factors:
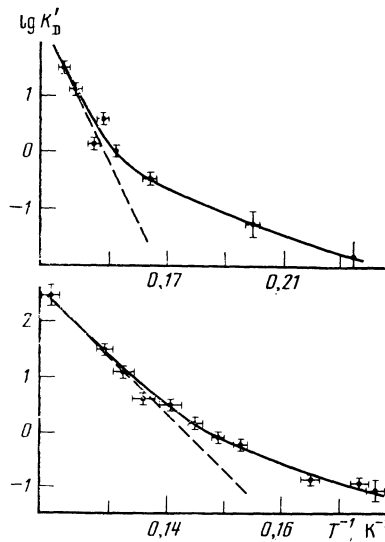

FIG. 5. Temperature dependence of the relative recombination rate constant for deuterium atoms in a D_2 matrix for specimen 2 (top, Table I) and specimen 5 (bottom).

$\log K_D^0 \sim -20$. This corresponds to an implausible value $\nu_D^0 \sim 10^2$ Hz for the frequency factor [see Eq. (8) below)].

4.2 Temperature dependence of the relative rate constant

We measured $K_D'(T)$ for ten specimens using an open atom guide. Because the concentration was unknown, these data cannot be compared directly with the absolute dependences $K_D(T)$; however, on the whole the two sets of results are quite similar. The curves $K_D(T)$ and $K_D'(T)$ have two characteristic temperature regions—at high temperatures they obey an activation dependence of the type (2), while at low temperatures (2) breaks down by an amount that varies from specimen to specimen.

This behavior is illustrated in Fig. 5, which plots $\log K_D'$ as a function of $1/T$ for two specimens in the series [$K_D'(T)$ is expressed in arbitrary units]. The solid curves give the best description of the experimental points for each specimen using an approximation of the type (3). Table I lists the results of this approximation for specimens with the largest number of temperature points. The resulting values of E_a and n are seen to be similar to the corresponding values for the absolute constants (4).

It should be noted that in this series of experiments, appreciable recombination was observed even at $T = 4.2$ K [the concentration decayed with a characteristic halflife

TABLE I. Parameters of the temperature dependence for the relative recombination rate constant for deuterium atoms in a D_2 matrix.

Specimen No.	Temperature interval, K.	E_a, K	n
1	5,90–7,26	240±30	9.6±1,9
2	4.25–7,45	240±10	8,6±0.5
3	5,50–7,52	240±30	9.9±1.2
4	5.65–8.20	210±30	10.5±1.5
5	5.67–8,34	230±30	10,3±1,0

* $K_D'(T) \infty \exp{(-E_a/T)} + \mathrm{const}\, T^n$.

$\tau_{1/2} \sim 10^5$ s]. The value of K'_D at 4.2 K was at least five orders of magnitude greater than the value found by extrapolating the high-temperature approximation Eq. (2) for $K'_D(T)$.

5. COMPARISON OF THE RECOMBINATION RATES FOR HYDROGEN AND DEUTERIUM ATOMS IN H₂ AND D₂ CRYSTALS

The absolute recombination rate constant K_H for atomic hydrogen in an H_2 matrix was measured for several specimens by using a closed atom guide at $T = 4.4$ K. The result was

$$\lg K_H(4,40) = -22,8 \pm 0,2. \tag{5}$$

The initial concentration of H atoms in these specimens reached $8 \cdot 10^{18}$ cm^{-3}. These measurements enabled us to deduce absolute values K_H [cm^3/s] from the temperature dependence $K_H(T)/K_H(4.2)$ found previously in Refs. 5 and 6. The preexponential factor for the activation portion of the curve $K_H(T)$ was found to be

$$\lg K_H^0 = -12.4 \pm 1.0. \tag{6}$$

For $T < 4$ K, we obtained $K_H(T) = AT$ with

$$A = (2 \pm 1) \cdot 10^{-24} \text{ cm}^3/\text{s} \cdot \text{K}. \tag{7}$$

Figure 6 compares the dependences $K_H(T)$ and $K_D(T)$ schematically. The dashed curves show the possible errors in the absolute values K_H due to errors in deducing the absolute values using (5). The heavy dark portion on the temperature curve $K_D(T)$ corresponds to the absolute values of K_D, while the dashed portion shows the relative values K'_D, assuming specimens with initial concentrations $C_D = 10^{-3} - 10^{-2}$ ($3 \cdot 10^{19} - 3 \cdot 10^{20}$ cm^{-3}). We see from Fig. 6 that the two curves are similar in many respects—in both cases, the activation region at higher temperatures is replaced by a weaker dependence as T decreases. However, the quantitative differences are very significant—the activation energy for D in D_2 is more than twice as large as for H in H_2; the preexponential factor K_D^0 is almost three orders of magnitude greater than K_H^0; at low temperatures, K_D depends on T much more strongly than $K_H(T)$, which is linear; the values K_H (4.2) are two to three orders of magnitude larger than K_D (4.2). Moreover, unlike the case of D in D_2, the
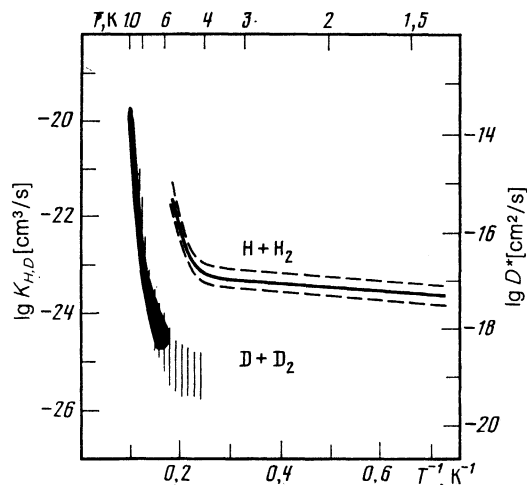

FIG. 6. Temperature dependence of the recombination rate constants for hydrogen atoms in an H_2 matrix and deuterium atoms in a D_2 matrix. The vertical axis on the right gives the recombination diffusion coefficient D^* [see Eq. (8)].

values of K_H for the H–H_2 system are reproducible from one specimen to another.

6. DISCUSSION

We have already noted that recombination of atoms in a molecular matrix becomes possible only if the atoms approach one another closely by diffusion. If we assume that the recombination diffusion coefficient D^* is constant throughout the crystal, then it is related to the recombination rate constant by[16]

$$K = 4\pi r_0 D^*, \tag{8}$$

where r_0 is the "reaction radius"; in our case we can set $r_0 = a$, since it is natural to assume that two atoms occupying adjacent lattice sites inevitably form a molecule. The vertical axis on the right in Fig. 6 shows D^* calculated using (8).

The dependences $K_H(T)$ and $K_D(T)$ are both of the activation type at high temperatures. This indicates that at these temperatures, the atoms approach one another by thermally activated diffusion, whence $D(T) = D_0 \exp(-E/T)$. Using (4)–(6) and (8), we can calculate D_0 and the corresponding frequency factors $\nu^0 \approx 6D_0/a^2 \approx 3\pi a^2/2 \cdot K^0$, which

TABLE II. Thermally activated diffusion in hydrogen and deuterium crystals.

Crystal	Diffusing particle	Temperature interval, K	$\lg D_0^*$ cm²/s	$\lg \nu^0$, s⁻¹	E_a, K	Ref.
H₂	H	4.5–5.5	−6.0±1.0 *	9.8±1.0 *	103±5	[5, 6]
	H	6–9	−1.5	14.3	195±10	[17] **
	H₂	10–14	−2.5	13.3	195±10	[18]
D₂	D	7.5–9.5	−2.2±1.5	13.8±1.5	270±30	this paper
	D₂	9–17	−3.4	12,4	276±20	

*Results of this paper
**Results of Leach *et al.* cited in Ref. 17.

are listed in Table II together with the activation energy E. For comparison, Table II also lists published values for self-diffusion processes in H_2 and D_2 crystals obtained from NMR studies. We see that the preexponential factor D_0 and the activation energy for deuterium atoms in a D_2 crystal are virtually identical to the corresponding values for self-diffusion of D_2, and the frequency ν_D^0 is comparable in order of magnitude to the Debye frequency of the crystal. This suggests that the activated diffusion mechanism involves vacancies.

We note that for H in H_2 the preexponential factor ν_H^0 is abnormally small, and in addition the activation energy also differs greatly from the data of Leach *et al.* listed in Table II. One possible explanation for the anomalously small values of ν_H^0 might be that they reflect a tunnel vacancy diffusion mechanism for $T = 4.5$–5.5 K. At higher temperatures, super-barrier atom-vacancy exchange processes may become dominant, which in principle could explain the discrepancy with the data of Leach *et al.* However, we note that the vacancy diffusion rate in the H_2 crystal would have to be very high to account for the observed recombination rates. It therefore seems quite likely that the discrepancy is due to some other factor. We will give a plausible explanation below which is based on considering the contribution from two-phonon quantum diffusion of hydrogen atoms at higher temperatures.

As we have already noted, the dependence $K_D(T)$ at *low temperatures* is stronger than $K_H(T)$, which is linear. The stronger dependence can be understood on the basis of the Kagan-Maksimov-Prokof'ev theory of quantum diffusion in irregular systems.[7]

In perfect crystals, an impurity atom can become delocalized by a quasiparticle moving in a band of width Δ, say. However if the deformation δ of the atomic energy levels at adjacent lattice sites due to the interaction of the atoms with defects and other atoms satisfies $\delta \gg \Delta$, the atoms are localized and can escape only if an atom-phonon interaction happens to make the energies of the levels coincide. If $\delta \gtrsim \delta_* \approx 30\hbar\omega(kT/\hbar\omega)^2$, one-phonon interactions are the most important; otherwise, two-phonon interactions dominate (here ω is the Debye frequency).

The above situation must always occur when atoms approach one another by diffusion, because the deformation of the atomic levels increases with proximity. The atoms can move quite rapidly when they are far apart, but when they start to approach one another ($\delta < \delta_*$), the probability of a tunneling jump caused by diffusion processes falls off as

$$W_{II} \approx 10^6 (\Delta/\delta)^2 \omega (kT/\hbar\omega)^9.$$

However, at shorter distances ($\delta \gtrsim \delta_*$), one-phonon processes become dominant and tend to decrease the distance further:

$$W_I \sim (\Delta^2\delta^2/\omega^4) T.$$

The effective recombination rate in this case depends on the time required to cross the "bottleneck" near $\delta \sim \delta_*$. If the

magnitude of the level deformations near the bottleneck is independent of T in some interval (e.g., due to the discreteness of the atomic positions in the lattice) then $K(T) = AT$. This is apparently what happens for hydrogen atoms in an H_2 matrix, for which the observed rate of recombination diffusion for $T < 4$ K is at least three orders of magnitude less than the average rate of spatial diffusion in the crystal.[8] The following points should be noted here. First, one can have $\delta > \delta_*$ at low temperatures for H atoms in an H_2 matrix, for which quantum diffusion is observed, because δ_* in this case is just a few degrees. Second, the above analysis implies that the characteristic magnitude of δ associated with H–H interactions should be greater than the energy level deformations caused by interactions of H with other lattice defects. This explains why the K_H values for different specimens are reproducible.

The situation for deuterium is radically different, apparently because the deformations caused by atom-defect interactions are dominant and cause a significant scatter in the values $K_D(T)$ for low T. In this case there is no bottleneck, and the spatial diffusion should be comparable to the interdiffusion of the atoms. Furthermore, δ_* is typically ~ 10 K for deuterium atoms in D_2 at low temperatures 5–7 K, so that the condition $\delta > \delta_*$ is not likely to be satisfied. We therefore expect two-phonon processes to dominate throughout the temperature interval investigated; the rates for these processes are strongly temperature-dependent, $K_D \sim W_{II} \sim T^9$, in agreement with the observed $K(T)$ curves [Eqs. (3), (4)].

Differences in the values of δ for the different specimens could be responsible for the unequal values of the coefficient B in (4). The absolute value of B can be used to derive the estimate $(\Delta_D/\delta) \sim 10^{-(4-5)}$ for the band width for deuterium atoms in a D_2 matrix. Taking $\delta \sim 1$–10 K we obtain $\Delta_D \sim 10^{-5}$–10^{-3} K, which is much less than the estimate $\Delta_H \sim 10^{-2}$–1 K for H–H_2 deduced in Ref. 7 from the H atom recombination data.[5,6] We note that an estimate for Δ_H based on the absolute value of the coefficient A in (7) gives a value in agreement with the lower limit in the above estimate.

In view of the above discussion, it is clear that two-phonon processes may become dominant at low temperatures, even for quantum recombination of hydrogen atoms in an H_2 matrix. We therefore attempted to approximate the experimental curve $K_H(T)$ by the formula $K_H(T) = K_H^0 \exp(-E_a/T) + AT + BT^9$, which differs from the previous approximation[5,6] in containing the extra term BT^9. We found that the term BT^9 did not appreciably change the closeness of the approximation but did alter the parameters contained in the activation term: $\log K_H^0 = -7.6 \pm 3$, $E_a = 172 \pm 40$ K. These values give a reasonable result $\nu_H^0 \sim 10^{14}$ s^{-1} for the frequency and agree with the data cited in Ref. 17. We also have $\log A = -23.9 \pm 0.2$, $\log B = -28.9 \pm 0.5$. The ratio B/A can be used in principle to estimate the characteristic magnitude of the energy level deformations for H atoms as they approach one another. Indeed, we have $B/A \approx 10^6 \delta^{-4} \omega^{-4}$ according to the theory in Ref. 7, whence $\delta \sim 5$ K.

7. SPIN RELAXATION OF HYDROGEN ATOMS IN A PARA-H₂ CRYSTAL WITH QUANTUM DIFFUSION

7.1 Experimental method

We prepared H–H₂ specimens with different ortho and para compositions by condensing two independent beams (one H, the other H₂ with a specified relative concentration C_{ortho} of ortho-H₂) on a cold substrate. The concentration of ortho-H₂ impurity in the "pure" para-H₂ was $10^{-4} < C_{\text{ortho}} < 10^{-3}$. The initial relative atomic concentration was $C_H \sim 10^{-5}$ in all cases. Special measures were taken to prevent contamination with oxygen, both in the starting gas and in the growing matrix ($C_{O_2} < 10^{-6}$).

The relaxation time T_e was deduced by using an EPR spectrometer (3-cm range) to directly measure the population differences of the Zeeman energy levels for atomic hydrogen (see Fig. 7) after a perturbation taking the spin system out of thermal equilibrium. We note that regardless of how the EPR spectrum was recorded, the amplitudes of the hyperfine structure lines were proportional to the population differences for the 1–4 and 2–3 levels at the instant they were recorded.

In the experiment, we held the system for a time $\gg T_e \sim 10$–100 s before recording the EPR signal twice at maximum saturation (the two times were separated by an interval t). If the line is swept during a time $\ll T_e$, then the signal amplitude during the second sweep reflects the relaxation of the population difference of the level pair of interest during time t. In addition, our equipment enabled us to change the strength of the polarizing magnetic field H rapidly (over times $\ll T_e$) from 40 to 150% of the resonance value H_0. We were therefore able to maintain the system in a field $H \neq H_0$ during the time t the system relaxed and thereby study the relaxation rate T_e (H) as a function of the magnetic field.

7.2 Electron and nuclear relaxation of atomic hydrogen in a para-H₂ crystal

We found that the electron and nuclear relaxations give comparable contributions to the relaxation rate of the Zeeman sublevels at resonance for $1.5 \leqslant T \leqslant 4.5$ K. The easiest
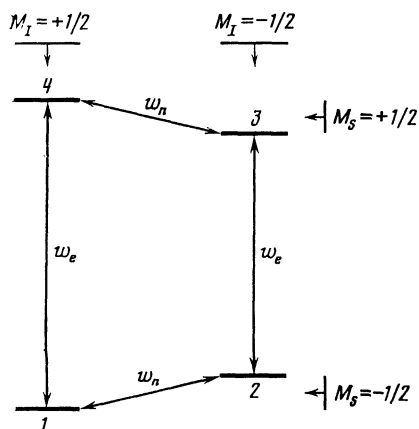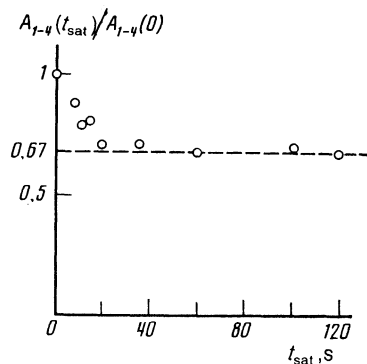
FIG. 8. Intensity of the EPR hyperfine line for atomic hydrogen corresponding to the 1–4 transition, as a function of the saturation time for the other hyperfine line.

way to distinguish the two contributions is as follows. First apply a large microwave power to saturate the system and ensure that the populations of the two Zeeman levels for one of the EPR transitions of interest (e.g., 2–3) are equal during the saturation time t_{sat}. Then change the magnetic field abruptly and record the other hyperfine structure line. In our experiment, saturation of the 2–3 transition caused the 1–4 transition to saturate, as can be seen from Fig. 8, and the situation was analogous when transition 1–4 was saturated prior to observing the 2–3 transition. The measured value for the maximum saturation of the second transition implies that the nuclear and electron relaxation rates are equal,

$$W_n/W_e = 1.06 \pm 0.26. \tag{9}$$

The longitudinal relaxation rate depends on the concentration of the atoms and molecules. As C_{ortho} decreases, the power required to saturate the EPR signal falls off steadily, which implies that the relaxation time increases as C_{ortho} drops. For specimens with $C_{\text{ortho}} < 0.03$ this is confirmed by direct measurements of T_e, which at $T = 1.6$ K can be approximated in order of magnitude by the relation $T_e C_{\text{ortho}} \sim 10^{-2}$ s. On the other hand, the atomic concentration has almost no effect on T_e. The relaxation may therefore

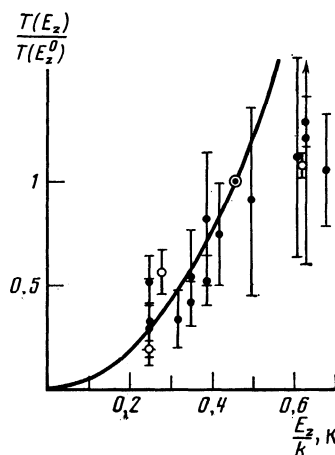FIG. 7. Zeeman energy levels for a hydrogen atom. The arrows show the relaxation transitions.

FIG. 9. Electron relaxation time vs splitting between the Zeeman sublevels. The curve plots the dependence $T_e \propto E_z^2$, the points show experimental values.

be attributed primarily to the interaction of the atoms with the ortho molecules:

$$(W_e)_{\text{H-ortho-H}_2} \gg (W_e)_{\text{H-H}}. \qquad (10)$$

Figure 9 plots the relaxation time as a function of the Zeeman splitting $E_Z \approx 2\mu_B H$ (where μ_B is the Bohr magneton) for $T = 1.6$ K; the results show $T_e(E_Z)/T_e(E_Z^0)$ as a function of E_Z/k, where $E_Z^0/k = 0.46$ K is the splitting at resonance. The dark circles correspond to saturation of one of the hyperfine lines under the assumption that $W_e = W_n$ throughout the range of magnetic fields. (We will examine the validity of this assumption below.) The open circles give values obtained by saturating both of the hyperfine lines in a control experiment (these results eliminate contributions from nuclear relaxation). In general, T_e increases monotonically with E_Z, and for $E_Z/k \lesssim 0.5$ K the relation

$$T_e \infty E_Z^2. \qquad (11)$$

approximates the experimental points fairly well. We also note that the dependence $T_e(E_Z)$ at $T = 4.5$ K has the same qualitative form.

The temperature dependence of the relaxation rate was analyzed at resonance ($H = H_0$). It should be noted that in spite of the large scatter in the low-temperature values ($1.5 \leqslant T \leqslant 4.5$ K), the dependence $W_e(T)$ was quite weak—if an approximation $W_e \sim T^n$ is assumed then $n = 0 - 1$.

7.3 Discussion

The fact that the relaxation is independent of the H atom concentration indicates that the spatial diffusion of the atoms is rapid and considerably faster than diffusion recombination. As was already noted, this situation is fully consistent with the theory of quantum diffusion in irregular systems[7]; it arises because the closer approach of atoms by tunneling is hindered by the increased deformation of the atomic energy levels at adjacent lattice sites (the deformation interaction between the atoms increases with proximity). If this interaction is stronger than the interaction of the atom with other lattice defects (e.g., ortho-H$_2$), the diffusion of the atoms toward each other may be substantially slower than their spatial diffusion. This makes it clear why the H-ortho-H$_2$ interaction rather than the H–H interaction gives the dominant contribution to W_e, whereas the relative magnetic moments for H and ortho-H$_2$ would lead one to expect $(W_e)_{\text{H-H}} \gg (W_e)_{\text{H-orthoH}_2}$ even when $C_H/C_{\text{ortho}} \sim 0.1$. However, the dipole interaction with the ortho-H$_2$ at intermediate distances is too weak to account for the observed values W_e, regardless of the relaxation mechanism. The requirement that an H atom and ortho-H$_2$ molecule approach one another during times $\lesssim T_e$ yields the lower bound $D \gtrsim a^2/C_{\text{ortho}} T_e \sim 10^{-13}$ cm^2/s for the spatial diffusion coefficient; this is much greater than the estimate $D^* \sim 10^{-17}$ cm^2/s for the recombination diffusion coefficient in Ref. 5.

Phonon relaxation mechanisms can be ruled out immediately for the following reasons. First, all multiphonon processes are strongly temperature-dependent, so that the same should be true of the relaxation rate, in conflict with the

experimental findings. Second, one-phonon processes, which have a linear temperature dependence $W_e \sim T$ (Ref. 20), lead to typical values $T_e \sim 10^5$ s even when the H atom and ortho-H$_2$ molecule occupy adjacent lattice sites. These times are at least three orders of magnitude longer than the experimental values. Finally, the dependence $W_e \sim H^2$ for one-phonon processes is just the opposite of the experimental behavior (11).

The dependence of W_e on the magnetic field can be understood in principle by using the Bloembergen mechanism of phononless relaxation,[21] provided the atoms are assumed to move coherently in a band of width $\Delta > E_Z$. The relaxation transition in this case is caused by fluctuations in the dipole interaction between an atom and an ortho-H$_2$ molecule, with a characteristic correlation time τ that is determined by the atomic diffusion:

$$W_e \sim (E_d/E_Z)^2 \tau^{-1} \quad (E_Z \tau/\hbar \gg 1),$$

where E_d is the characteristic energy for the dipole interaction. Comparison with the experimental data yields the estimate $\tau \leqslant 10^{-7}$ s, which corresponds to a diffusion coefficient $D > a^2/\tau \sim 10^{-8}$ cm^2/s $\gg D^*$. However, this model requires postulating an unreasonably large band width $\Delta/k > 1$ K for atomic hydrogen which conflicts with previous estimates.[7]

Following an idea suggested by Kagan, Shlyapnikov, and Prokof'ev in Ref. 22, we observe that phononless relaxation can occur when $\Delta \ll E_Z$, provided the energy level deformation $\delta = E_Z$ for an H atom near an orthomolecule is static. In this case, when the atom tunnels into an adjacent lattice cell the deformation of the levels is counterbalanced by the change in the Zeeman energy owing to the spin flip. Such deformations could in principle arise due to the anisotropic nature of the interaction between the ortho-H$_2$ and the atoms. Estimates show that because of the large number of atomic sites near an ortho-H$_2$ molecule and because of broadening due to other defects, these deformations form a quasicontinuous band of width $\Gamma/k \sim 1$ K. If $E_Z < \Gamma$, this mechanism yields

$$W_e \approx 10(E_d/E_Z)^2 (\Delta^2 C_{\text{ortho}}/\hbar\Gamma)$$

for the relaxation rate. If we substitute the experimental values, this formula gives an estimate consistent with a bandwidth $\Delta \lesssim 0.1$ K.

We note that equality $W_n = W_e$ can occur only if (11) holds. One can show that for magnetic fields $H < 10^5$ Oe, the nucleus of the hydrogen atom should relax through mixed states in the hyperfine level structure (1 and 3 in Fig. 7). Then $W_n(H) \approx \kappa^2 W_e(hA/2)$, where $\kappa = hA/2g_e\beta_e H$, while (11) implies that

$$W_e(hA/2) = W_e(H)(2E_Z/hA)^2.$$

We thus see that $W_n = W_e$ for all magnetic fields for which (11) is satisfied.

8. CONCLUSIONS

1. In this paper we have developed a new method for producing specimens which makes it possible to measure absolute atomic concentrations in molecular matrices to

within 40%. The initial concentrations of H atoms in an H_2 matrix and D atoms in a D_2 matrix were equal to 10^{19} and 10^{20} cm^{-3}, respectively.

2. The method can also be used to measure the temperature dependence of the absolute recombination rate constant for D atoms in a D_2 matrix for $T = 6$–10 K, and to deduce the absolute values from the temperature dependence found previously in Refs. 5, 6 for the relative recombination rates of H atoms in an H_2 matrix.

3. The relation

$$K_D = 10^{-8,2\pm1,5} \exp(-270\pm30/T) + BT^{8,8\pm0,6},$$

$$B = 10^{-30,8} - 10^{-32,4},$$

is consistent with the experimental results on the recombination rate constant for D atoms in a D_2 matrix throughout the temperature range investigated. The value of B differs from one specimen to the next and reflects the spread in the rate constants at low temperatures. Thus, at higher temperatures the recombination is determined by thermally activated diffusion of deuterium atoms, probably by a vacancy mechanism. At lower temperatures, the power-law dependence $K_D \propto T^9$ indicates that super-barrier quantum diffusion of D atoms involving two-phonon processes is dominant. In this case, the diffusion rate is limited by the deformation of the energy levels in atoms at adjacent lattice sites due to their interaction with crystal defects. The spread in K_D for different specimens at low temperatures can be ascribed to varying defect concentrations. A comparison of the experimental results with the theory in Ref. 7 gives an estimate $\Delta_D \sim 10^{-4}$ K for the band width for deuterium atoms in a D_2 crystal.

4. One-phonon quantum diffusion governs the temperature dependence of the absolute recombination rate constant for hydrogen atoms in an H_2 matrix in the region $T < 4$ K: $K_H(T) = 2\cdot10^{-24}T$. For $T \gtrsim 4.5$ K, one can describe $K_H(T)$ by the formula $K_H = 10^{-12.4}\exp(-103/T)$. However, this results in an anomalously small preexponential factor K_H^0, which indicates that at higher temperatures two-phonon quantum diffusion, which is strongly temperature-dependent, may contribute appreciably in addition to thermally activated diffusion. For these temperatures $K_H(T) = 10^{-7.6}\exp(-170/T) + 10^{-24}T + 10^{-29}T^9$.

5. We have demonstrated experimentally that the effective relaxation rate for the pair of D-atom energy levels corresponding to the central hyperfine line in the EPR spectrum is appreciably higher than for the other pairs of levels. We believe that such a situation can occur only if the nuclear relaxation rate for the D atoms in the D_2 crystal is comparable to the electron relaxation rate.

6. The EPR linewidth for D atoms in D_2 decreases steadily as the atomic concentration drops and (unlike the case for H in H_2) is independent of temperature.

7. We developed a technique for measuring the longitudinal spin relaxation times for atomic hydrogen in a para-H_2 crystal. The technique has the novel feature of employing a stationary EPR spectrometer operating at wavelengths in the 3-cm range.

8. We demonstrated experimentally that the electron and nuclear relaxation times are equal for hydrogen atoms in para-H_2. It was shown that this equality can occur only if the electron relaxation time increases with magnetic field as $T_e \sim H^2$, and the experimental dependence $T_e(H)$ is of this form. These findings indicate that the H atom spins in para-H_2 relax by a phononless mechanism.

9. We have shown that the primary contribution to the spin relaxation comes from the interaction of the hydrogen molecule with residual ortho-H_2 molecules ($C_{ortho} \sim 10^{-4}$–10^{-3}) and not from their interaction with other atoms ($C_H \sim 10^{-5}$). This is possible only if the spatial diffusion of the H atoms in the crystal is rapid: $D \gtrsim 10^{-13}$ cm^2/s. Such values are at least three orders of magnitude greater than the rate at which the atoms diffuse toward one another, as estimated from the recombination data.

[1] A. F. Andreev and I. M. Lifshits, Zh. Eksp. Teor. Fiz. **56**, 2057 (1969) [Sov. Phys. JETP **29**, 1107 (1969)].

[2] V. N. Grigor'ev, B. N. Esel'son, V. A. Mikheev, and E. E. Shul'man Pis'ma Zh. Eksp. Teor. Fiz. **17**, 25 (1973) [JETP Lett. **17**, 16 (1973)].

[3] Yu. Kagan and L. A. Maksimov, Zh. Eksp. Teor. Fiz. **65**, 622 (1973) [Sov. Phys. JETP **38**, 307 (1973)].

[4] V. A. Mikheev, Doctoral Dissertation, Khark. Fiz. Tekh. Inst. Nizk. Temp., Akad. Nauk UkrSSR, Khar'kov (1985).

[5] A. Ya. Katunin, I. I. Lukashevich, S. T. Orozmamatov, V. V. Sklyarevskiĭ, V. V. Suravev, V. V. Filippov, N. I. Filippov, and V. A. Shevtsov, Pis'ma Zh. Eksp. Teor. Fiz. **34**, 375 (1981) [JETP Lett. **34**, 357 (1981)].

[6] A. V. Ivliev, A. Ya. Katunin, I. I. Lukashevich, V. V. Sklyarevskiĭ, V. V. Suraev, V. V. Filippov, N. I. Filippov, and V. A. Shevtsov, Pis'ma Zh. Eksp. Teor. Fiz. **36**, 391 (1982) [JETP Lett. **36**, 472 (1982)].

[7] Yu. M. Kagan and L. A. Maksimov, Zh. Eksp. Teor. Fiz. **84**, 792 (1983) [Sov. Phys. JETP **57**, 459 (1983)]; Yu. M. Kagan, L. A. Maksimov, and N. V. Prokof'ev, Pis'ma Zh. Eksp. Teor. Fiz. **36**, 204 (1982) [JETP Lett. **36**, 253 (1982)].

[8] A. S. Iskovskikh, A. Ya. Katunin, I. I. Lukashevich, V. V. Sklyarevskiĭ, and V. A. Shevtsov, in: Proc. All-Union Seminar on Optical Alignment of Atoms and Molecules, Leningrad (1986), p. 188.

[9] A. S. Iskovskikh, A. Ya. Katunin, I. I. Lukashevich, V. V. Sklyarevskiĭ, and V. A. Shevtsov, in: Voprosy Atomnoĭ Nauki i Tekhniki, Vol. 4(25) (Topics in Atomic Science and Technology) (1983), p. 79.

[10] A. S. Iskovskikh, A. Ya. Katunin, I. I. Lukashevich, V. V. Sklyarevskiĭ, and V. A. Shevtsov, ibid, Vol. 4(29) (1984), p. 112.

[11] C. K. Jen, S. N. Foner, and L. Cochran, Phys. Rev. **112**, 1169 (1958).

[12] E. B. Gordon, A. A. Pel'menev, O. F. Pugachev, and V. V. Khmelenko, Pis'ma Zh. Eksp. Teor. Fiz. **37**, 237 (1983).

[13] M. Sharnoff and R. V. Pound, Phys. Rev. **132**, 1003 (1963).

[14] A. S. Iskovskikh, A. Ya. Katunin, I. I. Lukashevich, V. V. Sklyarevskiĭ, and V. A. Shevtsov, Pis'ma Zh. Eksp. Teor. Fiz. **42**, 26 (1985) [JETP Lett. **42**, 30 (1985)].

[15] A. S. Iskovskikh, A. Ya. Katunin, I. I. Lukashevich, and V. A. Shevtsov, Review, TsNIIAtominform., Moscow (1986).

[16] G. Eyring, S. G. Lin, and S. M. Lin, Basic Chemical Kinetics, Wiley, New York (1980).

[17] J. R. Gaines, T. R. Tsugawa, and P. C. Souers, Phys. Rev. Lett **42**, 1717 (1979).

[18] R. F. Buserak, M. Chan, and H. Meyer, J. Low Temp. Phys. **28**, 415 (1977).

[19]F. Weinhaus, H. Meyer, and S. M. Myers, Phys. Rev. **B7**, 2948 (1973).

[20]A. Abragam, *The Principles of Nuclear Magnetism*, Clarendon Press, Oxford (1961).

[21]N. Bloembergen, E. M. Purcell, and R. V. Pound, Phys. Rev. **73**, 679 (1948).

[22]Yu. M. Kagan, N. V. Prokof'ev, and G. V. Shlyapnikov, in: Proc. All-Union Seminar on Optical Alignment of Atoms and Molecules, Leningrad (1986), p. 192.

Translated by A. Mason